Lateral Diffusion of Small Compounds in Human Stratum Corneum and Model Lipid Bilayer Systems

Mark E. Johnson,*David A. Berk,# Daniel Blankschtein,* David E. Golan,§
Rakesh K. Jain,# and Robert S. Langer*

*Department of Chemical Engineering, Massachusetts Institute of Technology, Cambridge, Massachusetts 02139, #Department of Radiation Oncology, Massachusetts General Hospital and Harvard Medical School, Boston, Massachusetts 02114, and §Departments of Biological Chemistry and Molecular Pharmacology and of Medicine, Harvard Medical School and Brigham and Women's Hospital, Boston, Massachusetts 02115 USA

ABSTRACT An image-based technique of fluorescence recovery after photobleaching (video-FRAP) was used to measure the lateral diffusion coefficients of a series of nine fluorescent probes in two model lipid bilayer systems, dimyristoylphosphatidylcholine (DMPC) and DMPC/cholesterol (40 mol%), as well as in human stratum corneum–extracted lipids. The probes were all lipophilic, varied in molecular weight from 223 to 854 Da, and were chosen to characterize the lateral diffusion of small compounds in these bilayer systems. A clear molecular weight dependence of the lateral diffusion coefficients in DMPC bilayers was observed. Values ranged from 6.72×10^{-8} to 16.2×10^{-8} cm^2/s, with the smaller probes diffusing faster than the larger ones. Measurements in DMPC/cholesterol bilayers, which represent the most thorough characterization of small-solute diffusion in this system, exhibited a similar molecular weight dependence, although the diffusion coefficients were lower, ranging from 1.62×10^{-8} to 5.60×10^{-8} cm^2/s. Lateral diffusion measurements in stratum corneum–extracted lipids, which represent a novel examination of diffusion in this unique lipid system, also exhibited a molecular weight dependence, with values ranging from 0.306×10^{-8} to 2.34×10^{-8} cm^2/s. Literature data showed that these strong molecular weight dependencies extend to even smaller compounds than those examined in this study. A two-parameter empirical expression is presented that describes the lateral diffusion coefficient in terms of the solute's molecular weight and captures the size dependence over the range examined. This study illustrates the degree to which small-molecule lateral diffusion in stratum corneum–extracted lipids can be represented by diffusion in DMPC and DMPC/cholesterol bilayer systems, and may lead to a better understanding of small-solute transport across human stratum corneum.

INTRODUCTION

Over the past two decades, lateral diffusion in phospholipid bilayer systems has been extensively studied by use of a variety of experimental and theoretical techniques. The majority of these studies have been performed with the ultimate purpose of developing a better understanding of the fundamental and practical aspects of lateral diffusion in cell membranes. As such, these studies have focused on the diffusion of lipids and integral membrane proteins and on the relationships between lateral diffusion rates and the probe's intrinsic properties, such as molecular size and shape (Clegg and Vaz, 1985; Saffman and Delbrück, 1975). For example, integral protein diffusion has been found to exhibit a weak dependence on molecular size and is effectively described by use of existing continuum theories (Clegg and Vaz, 1985; Saffman and Delbrück, 1975). The effects of temperature, cholesterol content, and lipid tail length on the diffusion of lipid probes in model bilayer systems have also been effectively evaluated experimentally and theoretically (Almeida et al., 1992; Clegg and Vaz, 1985; Derzko and Jacobson, 1980; Rubenstein et al., 1979; Tocanne et al., 1989; Vaz et al., 1985).

In contrast, lateral diffusion in the lipid multibilayers of the stratum corneum (SC), the outermost layer of the skin, which constitutes the primary barrier to solute transport (Scheuplein and Blank, 1971), has been essentially unexplored despite the tremendous attention paid to SC transport. A better understanding of transdermal transport will facilitate the development of, for example, therapeutically effective drug delivery systems. To this end, measurements have been made of the SC permeability of more than 100 compounds, almost all of which are lipophilic and smaller than 500 Da in molecular weight (Flynn, 1990; Johnson et al., 1995a; Kasting et al., 1992). These compounds diffuse through the SC primarily via the interkeratinocyte lipids, which include ceramides, fatty acids, and sterols but essentially no phospholipids (Lampe et al., 1983). Detailed studies with electron microscopy (Hou et al., 1991; Madison et al., 1987) and small-angle x-ray diffraction (Bouwstra et al., 1991; Friberg and Osborne, 1985) have further revealed that the SC lipids exist in the form of multibilayers.

Comparisons of the molecular weight dependence of SC permeabilities have been made with transbilayer permeability measurements of various phospholipid bilayer systems (Potts and Guy, 1992; Scheuplein and Blank, 1971). These studies have shown that the molecular weight dependence of SC permeation of small, lipophilic drugs is strong and is similar to that exhibited by small, mostly hydrophilic compounds diffusing across phospholipid bilayers. In contrast, little attention has been devoted to the potential importance

Received for publication 3 May 1996 and in final form 1 August 1996.

Address reprint requests to Dr. Robert Langer, Department of Chemical Engineering, Massachusetts Institute of Technology, Cambridge, MA 02139. Tel.: 617-253-3107; Fax: 617-258-8827; E-mail: rlanger@mit.edu.

0006-3495/96/11/2656/13 $2.00

of lateral diffusion in SC transport, even though lateral and transbilayer diffusion are different processes and occur at significantly different rates (Diamond and Katz, 1974; Lange-Lieckfeldt and Lee, 1992). This lack of attention is largely due to the unavailability of experimental data on the lateral diffusion coefficients of compounds of any size (with the exception of molecular oxygen (Hatcher and Plachy, 1993)) in stratum corneum–extracted (SCE) bilayers and on the lateral diffusion coefficients of small probes (<500 Da) in other bilayer systems.

We explore lateral diffusion in SCE lipid bilayers by using the technique of image-based fluorescence recovery after photobleaching (video-FRAP) to measure the diffusion coefficients of a series of nine fluorescent probes of various molecular weights (223–854 Da) in SCE lipids. Diffusion of these nine probes is also measured in two model lipid systems, dimyristoylphosphatidylcholine (DMPC) and DMPC/cholesterol (40 mol%, referred to hereafter as DMPC/cholesterol). The goals of this paper are to 1) characterize experimentally lateral diffusion in SCE bilayers, 2) characterize experimentally lateral diffusion of small lipid and nonlipid probes in DMPC and DMPC/cholesterol model bilayer systems, 3) determine the molecular weight dependence of lateral diffusion in DMPC and DMPC/cholesterol model bilayer systems, using our data supplemented with available literature data to extend the size range to smaller probes, and 4) determine the molecular weight dependence of lateral diffusion in SCE bilayers by using our data as well as the diffusion coefficient of a previously examined probe (Hatcher and Plachy, 1993).

MATERIALS AND METHODS

Materials

The fluorescent probes examined in this paper were obtained from Molecular Probes (Eugene, OR) and used without further purification. The structures of these probes, namely, (*a*) 4-(dimethylaminocinnamylidene)-malononitrile (DACM, 223 Da), (*b*) 4,4-difluoro-1,3,5,7,8-pentamethyl-4-bora-3a, 4a-diaza-s-indacene (BOD, 262 Da), (*c*) 4-(*N*, *N*-dioctyl)amino-7-nitrobenz-2-oxa-1,3-diazole (NBD-dioct, 405 Da), (*d*) 4,4-difluoro-5,7-dimethyl-4-bora-3a, 4a-diaza-s-indacene-3-hexadecanoic acid (BOD-FA, 474 Da), (*e*) *N*-(4, 4-difluoro-5, 7-dimethyl-4-bora-3a, 4a-diaza-s-indacene-3-pentanoyl)sphingosine (BOD-Cer, 602 Da), (*f*) 4-(*N*, *N*-dihexadecyl)amino-7-nitrobenz-2-oxa-1,3-diazole (NBD-dihexdec, 629 Da), (*g*) cholesteryl 12-(*N*-methyl-*N*-(7-nitrobenz-2-oxa-1, 3-diazol-4-yl)amino)dodecanoate (NBD-Chol, 761 Da), (*h*) cholesteryl 4,4-difluoro-5,7-dimethyl-4-bora-3a, 4a-diaza-s-indacene-3-dodecanoate (BOD-Chol, 787 Da), and (*i*) *N*-(7-nitrobenz-2-oxa-1, 3-diazol-4-yl)-1,2-dipalmitoyl-sn-glycero-3-phosphoethanolamine (NBD-PE, 854 Da), are shown in Fig. 1. The wavelengths of the peak absorptions and emissions of these probes are listed in the caption of Fig. 1.

DMPC was obtained from Avanti Polar Lipids (Alabaster, AL) and stored in chloroform at −20°C. Cholesterol was obtained from Sigma Chemical (St. Louis, MO) and also stored at −20°C. All lipids were used without further purification.

SC lipids were extracted from human cadaver skin. The skin was from the chest, back, and abdominal regions and was obtained from local hospitals and the National Disease Research Institute (Philadelphia, PA). Cadaver skin was generally harvested within 24 h. Note that the SC lipid composition is fairly uniform for various body sites (Lampe et al., 1983). The skin was stored at −80°C until it was used. The epidermis was separated from the full-thickness tissue after immersion in 60°C water for 2 min. We then separated the SC from the heat-stripped epidermis by soaking the epidermis in a 0.5% trypsin solution overnight at 5°C (Anderson et al., 1988). The SC was cleaned with distilled water, rinsed in cold hexane to remove exogenous lipids, and lyophilized for 24 h or more to remove all water. Dried SC was cut into pieces of approximately 10 mg, weighed, and placed in a 7-ml vial with a ground glass cap. 5 ml of chloroform:methanol (2:1 v/v) were added to the vial. After at least 24 h, the delipidized SC (specifically, the remaining keratinocytes) was removed, lyophilized, and again weighed (Anderson et al., 1988). We determined the amount of lipids in the vial by taking the difference between the weights of the SC before and after delipidization. Typical lipid contents of the SC were 10–20% on a weight basis. Extracted SC lipid solutions were stored at −20°C until they were used.

Sample preparation

We prepared the DMPC and DMPC/cholesterol multibilayers with the appropriate probes by first combining the lipids and the probe in chloroform. The lipid-to-probe mole ratio was at least 1000. The solvent was removed by rotary evaporation followed by lyophilization. Milli-Q water heated to 45°C was added to the lipid film and vigorously mixed to produce an overall lipid concentration of ~10 mg/ml. The resulting liposome solutions were annealed at 45°C under a nitrogen atmosphere for 1 h. 10 μl of solution, representing 100 μg of total lipids, were placed on a microscope slide cover slip and dried for at least 4 h at 45°C. We finally hydrated the lipid films by placing the cover slips upon a microscope slide with a 10-μl drop of phosphate-buffered saline (pH 7.4, 10 mM phosphate, 137 mM NaCl). The cover slip was sealed with silicone paste (Baxter SP, #S9003-1) to prevent water evaporation (Almeida et al., 1992). Sealed samples were annealed at 45°C overnight and utilized within three days. Large multibilayer liposomes were selected by inspection with the FRAP video system, which is described below.

Extracted SC lipid solutions were combined with the fluorescent probes in chloroform:methanol (2:1 v/v). The lipid-to-probe mole ratio was 1000. 50 μg of lipids in solution were placed upon a microscope slide cover slip through successive application of a small amount of solution and drying. Once all the lipids were deposited, the cover slips were dried under low pressure to ensure removal of all the solvent. We dehydrated the SC lipid films by placing the cover slips upon a microscope slide onto which a 10-μl drop of phosphate-buffered saline had been placed, sealed them with silicone paste to prevent water evaporation, and annealed them at 45°C overnight. Large lipid domains were selected by inspection with the FRAP video system.

Diffusion measurements

Diffusion coefficients were measured by the FRAP technique. The reliability of this method was previously established for the measurement of diffusion in gels and aqueous systems (Berk et al., 1993; Johnson et al., 1995b). Utilization of the image-based FRAP technique offers several advantages over that of the conventional photomultiplier FRAP technique, including a simplified solution to the two-dimensional diffusion equation (see Eqs. 1–4 below). Detailed knowledge about the size, shape, and radial intensity distribution of the laser-beam radius is not needed. Moreover, the image-based FRAP technique utilizes the fluorescence intensities measured at more than 10,000 spatial locations at each time point to yield the diffusion coefficient. This allows for the characterization of diffusion in heterogeneous media (Tsay and Jacobson, 1991).

The microscope slide was placed upon the stage of an upright microscope (Universal; Zeiss, Thornwood, NY), and the sample was examined with epi-illumination. A beam splitter allowed the samples to be either illuminated by a mercury-arc lamp (100-W lamp; Osram, Munich) with stabilized power supply and convection-cooled housing (models 68806 and 60000; Oriel Corp., Stratford, CT) or exposed to a laser pulse for fluoro-

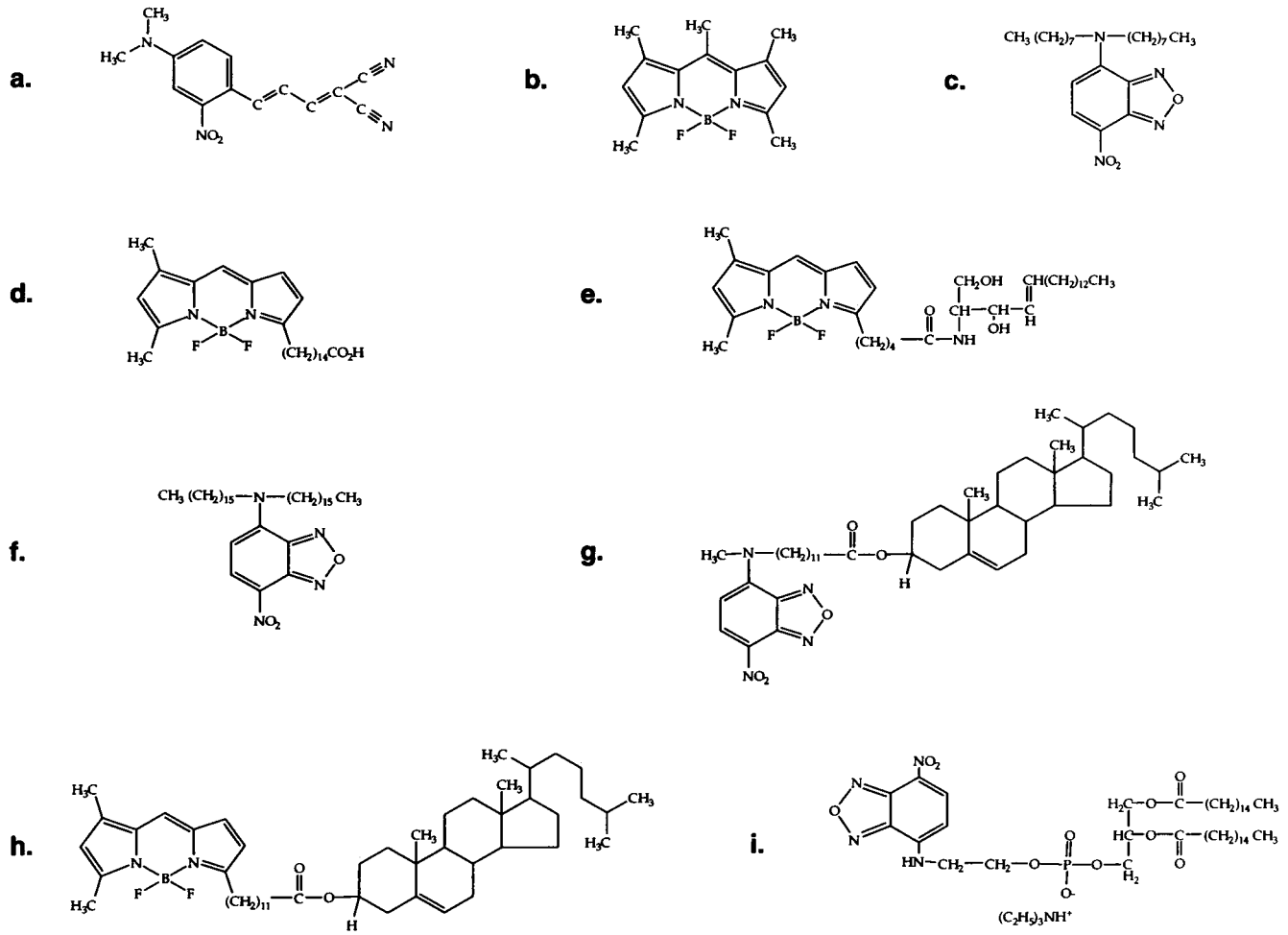

FIGURE 1 Chemical structures of the fluorescent probes examined in this paper: (*a*) DACM (223 Da), (*b*) BOD (262 Da), (*c*) NBD-dioct (404 Da), (*d*) BOD-FA (474 Da), (*e*) BOD-Cer (602 Da), (*f*) NBD-dihexdec (629 Da), (*g*) NBD-Chol (761 Da), (*h*) BOD-Chol (787 Da), and (*i*) NBD-PE (856 Da). The absorption peaks for these probes are 482, 491, 486, 474, 505, 485, 482, 504, and 460 nm, respectively, and their emission peaks are 577, 505, 543, 505, 511, 542, 540, 511, and 534 nm, respectively (Molecular Probes, Eugene, OR).

phore bleaching. An argon laser (model 2020; Spectra-Physics, Mountain View, CA) operated in the TEM_{00} mode, such that the beam intensity was radially symmetric and obeyed a Gaussian profile, was used for the fluorophore bleaching. The beam passed through a focusing lens into the microscope epi-illumination port and was focused by the objective onto the sample. A 40× objective (N.A. 0.65) produced a laser spot radius (that is, the Gaussian radius of the attenuated beam projected onto a fluorescent sample) of 5 μm. Experiments were performed at 27 ± 1.0°C. This warm temperature resulted from the heat produced by the arc lamp, computers, monitors, and other equipment in the small FRAP room. For those few cases when the temperature was below 26.5°C, an electric heat source placed near the microscope was used to elevate the temperature.

Samples were examined and suitable lipid structures were chosen by conventional epi-fluorescence illumination, an intensified CCD camera (model 2400; Hamamatsu, Japan), and a video monitor. The fluorescence image of the 33 μm × 33 μm region of each sample was digitized with a monochrome video digitization board (model S1V; EDT, Beaverton, OR). Only a portion (128 × 128 pixels) of the full (640 × 480 pixel) images was stored for analysis. The spatial sampling rates (that is, the vertical and horizontal distances between pixels) were determined with a stage micrometer (Edmund Scientific, Barrington, NJ). We performed FRAP experiments by briefly exposing each sample to the laser, typically for 10–100 ms, to produce a bleached spot on the sample. A longer exposure time of 200 ms was used for the probe DACM because this probe was found to be especially resistant to photobleaching. Under conventional epi-illumination, 50 postbleach images were obtained over the course of 20–120 s, depending on the diffusion coefficient of the probe/lipid system. The first 10 images were obtained at the maximum sampling rate of 30 images/s, and 10 or more additional images were obtained at one-tenth of the maximum sampling rate, or 3 images/s. Thirty additional images were obtained at rates suitable to the time scale of the experiment.

Analysis of FRAP data

Two-dimensional diffusion is described by Fick's second law:

$$\frac{\partial C(x, y, t)}{\partial t} = D\nabla^2 C(x, y, t), \tag{1}$$

where C is the concentration of the probe species, D is the lateral diffusion coefficient, t is time, and x and y are the two-dimensional spatial coordinates. The Fourier-transform representation of this partial differential equation is a simple ordinary differential equation, namely,

$$\frac{d\tilde{C}(u, v, t)}{dt} = -4\pi^2 D(u^2 + v^2)\tilde{C}(u, v, t), \tag{2}$$

where $\tilde{C}(u, v, t)$ is the Fourier transform of the concentration and u and v are the spatial frequency components. The solution of Eq. 2 is a simple exponential equation rather than the more complex and cumbersome solutions of Eq. 1. Specifically,

$$\tilde{C}(u, v, t) = \tilde{C}(u, v, 0)\exp(-4\pi^2 q^2 Dt), \quad (3)$$

where q represents the spatial frequencies and is given by $q^2 = u^2 + v^2$. The fluorescence intensity in Fourier space, $\tilde{I}(u, v, t)$, is related to the fluorophore concentration, $\tilde{C}(u, v, t)$, such that

$$\frac{\tilde{I}(u, v, t)}{\tilde{I}(u, v, 0)} = \frac{\tilde{C}(u, v, t)}{\tilde{C}(u, v, 0)} = \exp(-4\pi^2 q^2 Dt). \quad (4)$$

Equation 4 describes a complete dissipation of the photobleached pattern. However, the fluorophore pattern in some FRAP experiments performed with lipid bilayer systems exhibits an incomplete or biphasic recovery. We used a modified form of Eq. 4, based on the assumption of an immobile or slow component, to analyze the FRAP data and obtain the primary parameter of interest, D. Specifically,

$$\frac{\tilde{I}(u, v, t)}{\tilde{I}(u, v, 0)} = \epsilon + (1 - \epsilon)\exp(-4\pi^2 q^2 Dt), \quad (5)$$

where ϵ represents the immobile fraction.

Analyses of representative FRAP recovery profiles for each probe in each lipid system were also performed with a two-diffusion-coefficient model, namely,

$$\frac{\tilde{I}(u, v, t)}{\tilde{I}(u, v, 0)} = f_1 \exp(-4\pi^2 q^2 D_1 t) + (1 - f_1)\exp(-4\pi^2 q^2 D_2 t), \quad (6)$$

where D_1 and D_2 are the diffusion coefficients and f_1 represents the fraction of the probe diffusing in a regime characterized by D_1. Use of Eq. 6 proved statistically unnecessary for all but one of the probe/lipid systems, as we determined by using the F statistic, namely,

$$F_n = \frac{(\chi^2_{n-1} - \chi^2_n)(N-2n-1)}{2\chi^2_n}, \quad (7)$$

where χ^2_n is the chi-squared goodness-of-fit statistic for n diffusing components and N is the number of experimental data points (1000) (Wright et al., 1988). F_2 values less than the critical value of 3.0 indicated that analyses that used Eq. 6 did not result in a statistically significant improvement over those for which Eq 5 was used. However, the diffusion of one probe, BOD-Chol in SCE bilayers, did consistently exhibit F_2 values greater than 3.0 and is considered more thoroughly in the Discussion.

We obtained values of $\tilde{I}(u, v, t)$ from the real values of the digitized images by first subtracting each postbleach image from the prebleach image and then subjecting the result to a discrete Fourier transform (Berk et al., 1993). Artifacts associated with the discrete transform were minimized by a digital windowing technique, as previously described (Johnson et al., 1995b). Specifically, each differential image was padded at its edges (to a size of 256 × 256 pixels) and then multiplied by a two-dimensional windowing function that smoothly attenuated the intensity to zero at the boundaries. A two-dimensional fast-Fourier-transform algorithm was then applied to produce an array of complex coefficients corresponding to discrete spatial frequencies, $i\Delta u$ and $j\Delta v$ (where i and j ranged from −127 to 128). From each of the 50 postbleach images a total of 20 unique components were utilized for fitting to the decay equations (Eqs. 4–6). The components most useful for this purpose were the low-spatial-frequency components, although the lowest-frequency group was ignored because it does not decay. More frequencies were utilized in this study (20) than in earlier studies (8) because of the use here of a video digitization board that could acquire images at a sixfold faster rate. The faster sampling rate resulted in an increased signal-to-noise ratio of the higher frequencies, thus enabling more frequencies to be useful. The set of Fourier coefficients was then fitted to the decay equation with one, two, or three parameters (Eqs. 4–6) by use of a nonlinear least-squares algorithm, as described previously (Berk et al., 1993; Johnson et al., 1995b).

RESULTS

Diffusion in DMPC and DMPC/cholesterol lipid bilayers

Representative recovery plots of the recovery of the diffusion of BOD in DMPC, DMPC/cholesterol, and SCE lipid bilayers are shown in Fig. 2, where the Fourier coefficients, $\tilde{I}/\tilde{I}_o$, corresponding to the 20 lowest spatial frequencies from each of the 50 postbleach images, are plotted against frequency-scaled time, $4\pi^2 q^2 t$. Inasmuch as each component is scaled by its value in the first postbleach image, dissipation of the photobleached pattern is represented by a decay from 1 to 0. The recovery of BOD in DMPC is faster than in DMPC/cholesterol; hence its diffusion coefficient, 1.25×10^{-7} cm^2/s ($R = 0.998$), is greater than that in DMPC/cholesterol, 2.33×10^{-8} cm^2/s ($R = 0.989$). Fig. 2 also shows that the recovery profiles are all well represented by Eq. 5, from which the diffusion coefficient D and the immobile fraction ϵ were determined by a least-squares regression. The recovery profiles for the other eight probes in DMPC and DMPC/cholesterol lipid bilayers are qualitatively similar to those shown in Fig. 2 and are also well described by Eq. 5.

Results of the analyses for the nine fluorescent probes examined in DMPC bilayers are summarized in Table 1. The diffusion coefficients in DMPC, measured at 27°C, range from as large as 16.2×10^{-8} cm^2/s for DACM, the smallest probe, to 6.75×10^{-8} cm^2/s for NBD-Chol. The diffusion coefficient for NBD-PE is 6.88×10^{-8} cm^2/s. This value is in good agreement with previously reported values of the NBD-PE diffusion coefficient in DMPC lipid bilayers, which range from 4.3×10^{-8} cm^2/s (Galla et al., 1979) to 8.2×10^{-8} cm^2/s (Wu et al., 1977) (Table 2). [The lengths of the alkyl chains of the various NBD-PE probes used in previous studies were not all the same. The NBD-PE probe used in this and other studies (Balcom and Petersen, 1993; Paprica, 1994), NBD-dipalmitoylphosphatidylethanolamine, has an alkyl chain length of 16. NBD-dimyristoylphosphatidylethanolamine, with an alkyl chain length of 14, was also used (Vaz et al., 1985), whereas Almeida et al.(1992) used NBD-didecanoylphosphatidylethanolamine. At the time of the earlier studies (Chang et al., 1981; Derzko and Jacobson, 1980; Galla et al., 1979; Rubenstein et al., 1979; Wu et al., 1977), the NBD-PE probe that was commercially available (Avanti Polar Lipids, Alabaster, AL) had a slightly larger molecular weight of 880 Da. Inasmuch as previous studies showed that differences in alkyl tail length of a series of NBD-PE probes do not substantially affect the diffusion coefficient in distearoylphosphatidylcholine lipid bilayers because of the restrictions on the large headgroup in the more highly ordered headgroup region

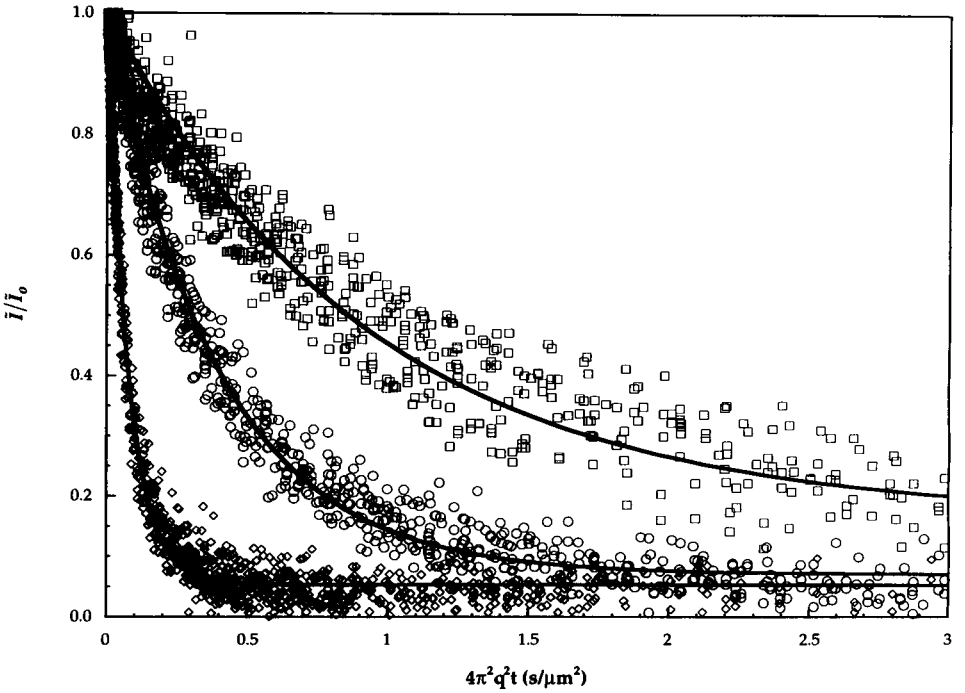

FIGURE 2 Recovery profiles of BOD in DMPC lipid bilayers (◇), DMPC/cholesterol lipid bilayers (○), and SCE lipid bilayers (□). The Fourier coefficients, corresponding to the 12 lowest spatial frequencies from each of the 50 postbleach images, are plotted against frequency-scaled time, $4\pi^2q^2t$. Because each component is scaled by its value in the first postbleach image, dissipation of the photobleached pattern is represented by a decay from 1 to 0. The lines were obtained by least-squares regression on the data, using Eq. (5).

(Vaz et al., 1985), the diffusion coefficients of these similar probes should be comparable.] The average immobile fractions of the probes in the DMPC bilayer experiments (Table 1) range from 2.6% to 4.6%, which are also in good agreement with the results of others (Balcom and Petersen, 1993). These favorable comparisons of our results with those in the literature confirm that video-FRAP is an effective and accurate method for measuring lateral diffusion in lipid bilayer systems.

Results of analyses for the nine fluorescent probes in DMPC/cholesterol bilayers are also summarized in Table 1. Values of the diffusion coefficients in DMPC/cholesterol, obtained at 27°C, range from 5.60×10^{-8} cm^2/s for DACM, the smallest probe, to 1.32×10^{-8} cm^2/s for NBD-Chol. Our value for the diffusion coefficient of NBD-PE in DMPC/cholesterol lipid bilayers, 1.62×10^{-8} cm^2/s, is also in good agreement with previously reported measurements of NBD-PE in DMPC bilayers with 40–50 mol% cholesterol: 1.1×10^{-8} cm^2/s at 30°C (Chang et al., 1981), 1.3×10^{-8} cm^2/s at 26°C (Rubenstein et al., 1979), 2×10^{-8} cm^2/s at 30°C (Wu et al., 1977), and 2.7×10^{-8} cm^2/s at 30°C (Almeida et al., 1992). Combined with the results obtained for NBD-PE diffusion in DMPC, these results confirm the ability of the video-FRAP technique to measure diffusion coefficients spanning a wide range of values. The immobile fractions of the probes in DMPC/cholesterol are 5–7% (±3%), except for DACM, which has an immobile fraction of 16% (±9%) because of the higher noise levels obtained with this probe. Table 1 also shows that the diffusion coefficient values in DMPC are all greater than those in DMPC/cholesterol. This finding is in agreement with the general findings of many others that the isothermal addition of cholesterol to fluid phase phospholipid bilayers (that is, at $T > T_m$, where T_m = 23.9°C for

TABLE 1 Diffusion coefficients and immobile fractions of low-molecular-weight probes in DMPC and DMPC/cholesterol (40 mol. %) bilayers

	DMPC			DMPC/Cholesterol (40 mol%)		
Probe	D (10^{-8} cm^2/s)	ε (%)	n	D (10^{-8} cm^2/s)	ε (%)	n
DACM	16.2 ± 2.0	4.6 ± 2.3	12	5.60 ± 1.5	16 ± 8.5	13
BOD	12.5 ± 1.3	2.6 ± 1.0	14	2.33 ± 0.20	6.5 ± 1.9	32
NBD-dioct	10.1 ± 1.2	4.8 ± 1.4	12	2.87 ± 0.38	5.2 ± 4.3	27
BOD-FA	7.89 ± 0.41	3.3 ± 1.0	20	1.92 ± 0.17	4.5 ± 1.9	36
BOD-Cer	7.52 ± 0.29	3.6 ± 0.4	16	1.88 ± 0.07	7.2 ± 2.8	24
NBD-dihexdec	7.80 ± 0.47	4.3 ± 1.2	16	1.65 ± 0.16	4.9 ± 1.9	26
NBD-Chol	6.75 ± 0.45	4.8 ± 1.7	11	1.32 ± 0.09	6.7 ± 1.5	14
BOD-Chol	7.24 ± 0.46	4.3 ± 0.6	12	1.69 ± 0.18	7.5 ± 3.2	27
NBD-PE	6.88 ± 0.59	4.1 ± 1.2	23	1.62 ± 0.16	6.5 ± 2.6	44

Values were measured at 27°C and are given as mean ± SD. n is the number of measurements.

TABLE 2 Summary of literature values of lipid and small-probe lateral diffusion coefficients in DMPC lipid bilayers

Probe	T (°C)	D^* (10^{-8} cm^2/s)	$D_c^{\#}$ (10^{-8} cm^2/s)	Reference
NBD-PE	30	5.9	5.9	(Almeida et al., 1992)
Nifedipine analog	47	130[§]	710	(Alper and Stouch, 1995)
NBD-citronello	29	4.8	5.0	(Balcom and Petersen, 1993)
NBD-PE	29	5.0	5.2	(Balcom and Petersen, 1993)
NBD-solanesol	29	5.3	5.5	(Balcom and Petersen, 1993)
NBD-dolichol	29	4.6	4.8	(Balcom and Petersen, 1993)
Tetracene	29	11	11	(Balcom and Petersen, 1993)
Rubrene	29	5.8	6.0	(Balcom and Petersen, 1993)
Benzene	47	280[§]	154	(Bassolino-Klimas et al., 1993)
NBD-PE	30	7.6	7.6	(Chang et al., 1981)
NBD-dodecanoic acid	24	7.2	11	(Derzko and Jacobson, 1980)
3,3′-Dihexyloxacarbocyanine iodide	33	8.2	7.7	(Derzko and Jacobson, 1980)
3,3′-Didodecanoylindocarbocyanine iodide	24	5.2	7.3	(Derzko and Jacobson, 1980)
3,3′-Dioctadecyloxacarbocyanine iodide	24	6.7	7.7	(Derzko and Jacobson, 1980)
3,3′-Dioctadecylindocarbocyanine iodide	24	8.4	9.8	(Derzko and Jacobson, 1980)
NBD-PE	24	6.3	7.7	(Derzko and Jacobson, 1980)
NBD-PE	30	4.3	4.3	(Kapitza et al., 1984)
NBD-Macrocyclic polyamide dimer	36	7.5	5.9	(Paprica, 1994)
NBD-Macrocyclic polyamide trimer	36	7.4	5.8	(Paprica, 1994)
NBD-PE	36	8.0	6.3	(Paprica, 1994)
NBD-Macrocyclic polyamide quatramer	36	6.3	5.0	(Paprica, 1994)
NBD-Macrocyclic polyamide pentamer	36	6.6	5.2	(Paprica, 1994)
NBD-Macrocyclic polyamide hexamer	36	4.2	3.3	(Paprica, 1994)
3,3′-Dioctadecyloxacarbocyanine iodide	29	6.9	7.4	(Peters and Cherry, 1982)
NBD-PE	26	4.8	5.7	(Rubenstein et al., 1979)
Oxygen	40	2700[‖]	1800	(Subczynski et al., 1991)
1-methylpyrene	30	55**	55	(Van den Zegel et al., 1984)
NBD-PE	30	5.3	5.3	(Vaz et al., 1985)
3,3′-Dioctadecyloxacarbocyanine iodide	30	5.5	5.5	(Wu et al., 1977)
NBD-PE	30	8.2	8.2	(Wu et al., 1977)

*Diffusion coefficients were measured with FRAP unless otherwise noted.

#Diffusion coefficient corrected to 30°C by use of either the activation energy reported in the same reference in which the diffusion coefficient measurement was reported or of the typical value of 7.4 kcal/mol (Almeida et al., 1992; Chang et al., 1981; Peters and Cherry, 1982; Van den Zegel et al., 1984).

§Average values of the calculated diffusion coefficients in a DMPC bilayer determined from a molecular dynamic simulation.

‖Calculated from measurements of the bilayer permeability P, with $D = P\delta/K$, where δ is the bilayer thickness and K is the bilayer/water partition coefficient, estimated from its octanol/water partition coefficient, $K_{o/w}$ (3.68; Hansch and Leo (1979)), by $K = K_{o/w}^{0.87}$. This value constitutes an upper estimate of the diffusion coefficient that is due to the resistance associated with crossing the bilayer headgroup region (Diamond and Katz, 1974).

**Measured with the fluorescence decay technique.

DMPC (Mabrey and Sturtevant, 1976)) produces a more ordered bilayer structure in which the diffusion coefficients are reduced. The diffusion coefficient of each probe in DMPC is consistently greater than that in DMPC/cholesterol, by an average factor of 4.3 (SD 18%).

Diffusion in SCE lipid bilayers

The recovery profile of BOD in SCE lipid bilayers is qualitatively similar to those for BOD diffusion in DMPC and DMPC/cholesterol bilayers (Fig. 2), except that it exhibits a significantly longer characteristic recovery time, which corresponds to a smaller value of the diffusion coefficient, 1.22×10^{-8} cm^2/s ($R = 0.980$). Fig. 2 also shows that there was incomplete recovery of BOD diffusion in SCE, with an immobile fraction of 27%. Importantly, this figure also shows that the recovery was fairly uniform, confirming that the fluorescence recovery process was governed by diffusion of a single population. The recovery profiles for DACM, NBD-dioct, NBD-dihexdec, and NBD-Chol were also uniform and are well described by Eq. 5. The diffusion coefficients and immobile fractions of these five probes in SCE bilayers are shown in Table 3. The diffusion coefficients of DACM, BOD, NBD-dioct, NBD-dihexdec, and NBD-Chol in SCE lipids range from as great as 2.34×10^{-8} cm^2/s for the smallest probe, DACM, to 3.06×10^{-9} cm^2/s for NBD-dihexdec. The immobile fractions of these probes vary from 17% to 32%. Similar immobile fractions (17–60%) have also been observed in other complex lipid systems, including multicomponent bilayers (Vaz et al., 1989, 1990), biological membranes characterized by slow diffusion ($D \leq 10^{-9}$ cm^2/s) (Cherry, 1979), and gel-phase phospholipid bilayers (Balcom and Petersen, 1993).

Recovery curves of BOD diffusion in SCE bilayers were analyzed with the two-diffusion-coefficient model, Eq. 6, because the F statistic, Eq. 7, revealed that Eq. 6 provides a statistically significant improvement in accuracy over Eq. 5. These results suggested that the majority of BOD-Chol,

TABLE 3 Diffusion coefficients and immobile fractions of low-molecular-weight probes in SCE bilayers

Probe	D (10^{-8} cm^2/s)	ϵ (%)	n
DACM	2.34 ± 0.41	17 ± 3.6	16
BOD	1.22 ± 0.17	27 ± 10	20
NBD-dioct	0.712 ± 0.20	19 ± 8.0	22
BOD-FA	*	*	27
BOD-Cer	*	*	29
NBD-dihexdec	0.306 ± 0.181	32 ± 20	12
NBD-Chol	0.385 ± 0.19	22 ± 12	16
BOD-Chol	0.125 ± 0.07#	22 ± 4.8#	22
NBD-PE	*	*	24

Values were measured at 27°C and are given as mean ± SD. n is the number of measurements.

*The fluorescence intensity recovery curves in Fourier space did not exhibit an exponential decay.

#Analyzed with Eq. 6. The two calculated diffusion coefficients were $0.125(\pm0.07) \times 10^{-8}$ and $1.59(\pm0.57) \times 10^{-8}$ cm^2/s, and the distribution coefficient was f_1 = 78%(±5%). That is, 78% of the probe appeared to diffuse at the slower rate and 22% at the faster rate.

78 ± 5%, diffused at a rate of 1.25×10^{-9} cm^2/s, whereas the remainder of the probe, 22%, exhibited a diffusion coefficient that was more than an order of magnitude greater, 1.59×10^{-8} cm^2/s. The recovery profiles for BOD-FA, BOD-Cer, and NBD-PE in SCE bilayers did not exhibit exponential decays, in contrast to the results for BOD (Fig. 2) and the other probes examined, and are considered further in the Discussion.

DISCUSSION

Molecular weight dependence of lateral diffusion in DMPC lipid bilayers

The measured diffusion coefficients of the nine probes in DMPC bilayers are shown in Fig. 3*a* plotted against the probe molecular weight. These data exhibit a molecular weight dependence, with the smaller probes tending to diffuse faster than the larger probes. The diffusion coefficient of the fastest probe, DACM, is 2.4-fold greater than that of the slowest probe, NBD-Chol. With respect to diffusion in DMPC bilayers, this change is dramatic. To illustrate the significance of this finding, consider the Saffman–Delbrück equation (Saffman and Delbrück, 1975), which effectively describes the diffusion of integral proteins in fluid-phase lipid bilayers, namely,

$$D = \left(\frac{k_bT}{4\pi\eta_0 h}\right)\left[\ln\left(\frac{\eta_0 h}{\eta r_c}\right) - \gamma_e\right], \qquad (8)$$

where k_b is Boltzmann's constant, T is temperature (303 K), η_o is the effective viscosity of the bilayer, η is the viscosity of the surrounding aqueous medium, h is the "height" of the protein, which is assumed to span the bilayer and is equivalent to the bilayer thickness (55 Å), r_c is the solute radius, and γ_e is Euler's constant (0.5772). When one uses a value of 0.75 P for η_o (Vaz et al., 1984) and 0.01 P for η (Bird et al., 1960) and assumes a specific gravity of 0.9, the Saffman–Delbrück equation predicts that a 470,000 Da probe, which has a molecular mass nearly 3 orders of magnitude greater than those of the probes that we have examined, would have a diffusion coefficient that is only 2.4-fold less than that of NBD-Chol. [We relate the molecular weights of the probes to their molecular volumes through $M = vN_ag$, where M is the molecular weight, v is the molecular volume, N_a is Avogadro's number, and g is the specific gravity. The specific gravity of the probes is taken to be a typical value for organic molecules, 0.9 (Weast, 1975).] Equation 8 illustrates that the diffusion coefficients of larger probes in DMPC bilayers exhibit a very weak dependence on probe size. In contrast, the diffusion coefficients of smaller compounds in DMPC bilayers increase dramatically with decreasing probe molecular weight (Fig. 3 *a* and the discussion below).

Fig. 3 *a* shows several cases, including the pair NBD-dihexdec and BOD-Cer as well as the pair BOD-Chol and NBD-Chol, in which a larger probe has an apparently greater diffusion coefficient than a smaller probe. However, these differences are not statistically significant at the 95% confidence level when the two-tailed Student's t-test is used. Table 1 and Fig. 3 *a* also show that the standard deviation of the DACM diffusion coefficient is unusually large (13%). This is due, in part, to the photostability of DACM, which makes it more resistant to bleaching than the other probes and, hence, results in weaker bleach spots and noisier recovery profiles.

Also shown in Fig. 3 *a* is the dependence of the diffusion coefficient on molecular weight, obtained by least-squares regression on the DMPC data with the equation

$$D = aM^{-b} + \left(\frac{k_bT}{4\pi\eta_0 h}\right)\left[\ln\left(\frac{\eta_0 h}{\eta r_c}\right) - \gamma_e\right], \qquad (9)$$

where M is the probe molecular weight and a and b are empirically determined parameters. The probe radius, r_c, in the second term of Eq. 9 and M are related by $r_c = [M/(\pi h N_a \rho)]^{1/2}$, where ρ is the solute density. The remaining parameters in Eq. 9 were described above. Equation 9 combines a term exhibiting a strong molecular weight dependence, aM^{-b}, with a term exhibiting a weak size dependence as given by the Saffman–Delbrück relationship (Eq. 8). The first term, aM^{-b}, which has been used effectively to describe the diffusion of small solutes in various biological tissues, including human stratum corneum permeabilities (Anderson and Raykar, 1989), red blood cells (Lieb and Stein, 1986), and stroma (Cooper and Kasting, 1987), is included to capture the dramatic increase in diffusion coefficients as the probe molecular weight decreases below ~400 Da, and the second term is included to account for the weaker molecular weight dependence that appears to begin at ~500 Da. These terms are effectively used in an additive manner because, in the low-molecular-weight regime, the contribution of the first term is much greater than that of the second, whereas in the high-molecular-weight regime the contribution of the first term becomes insignificant

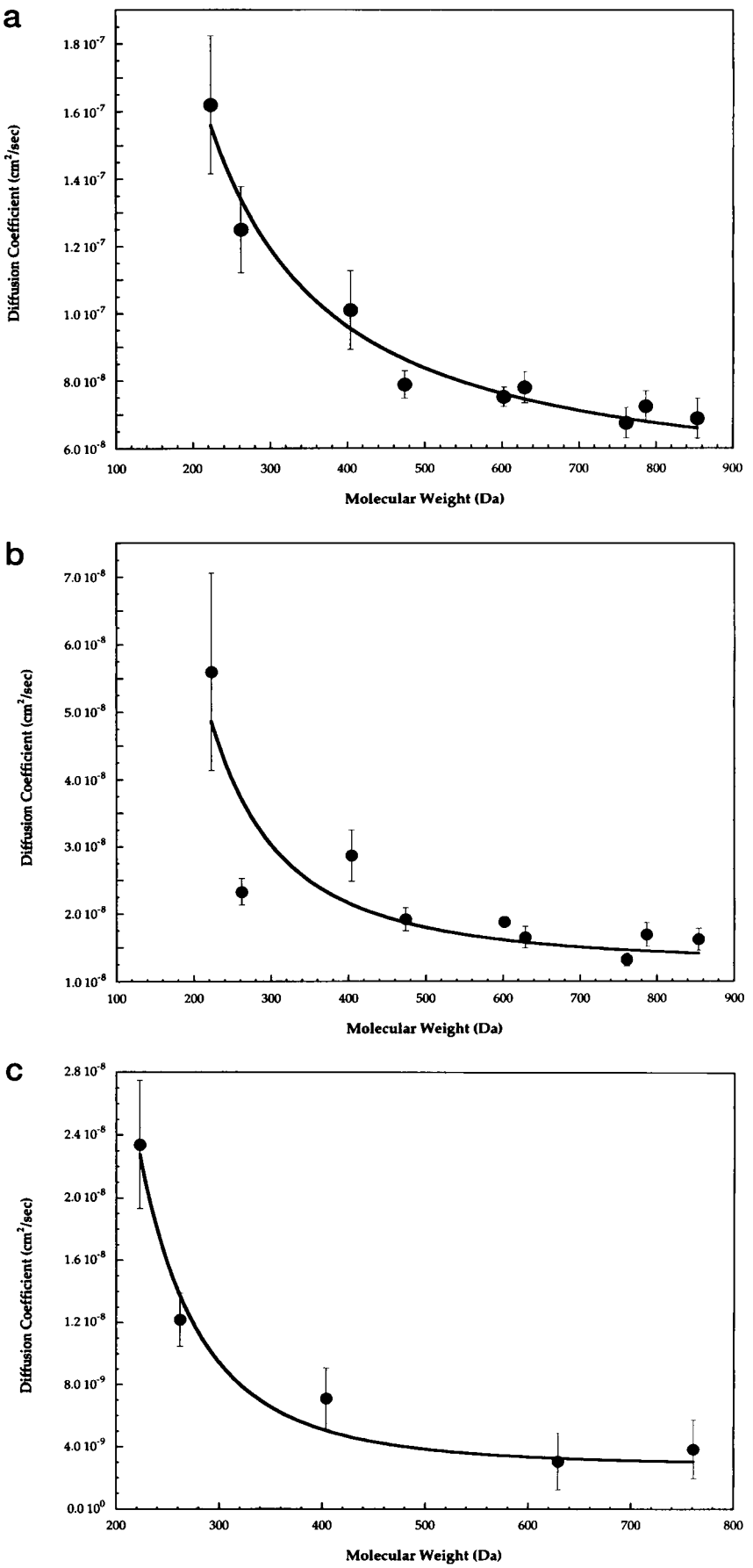

FIGURE 3 Diffusion coefficients of the fluorescent probes in (*a*) DMPC, (*b*) DMPC/cholesterol, and (*c*) SCE lipid bilayers, as measured by the video FRAP technique at 27°C, versus the probe molecular weight. These data exhibit a distinct molecular weight dependence, with the diffusion coefficients decreasing with increasing probe molecular weight. The curves represent the semiempirical model (Eq. 9), which combines the strong molecular weight dependence of free-volume theory in the lower-molecular-weight regime with the weak molecular weight dependence of continuum theories in the larger-molecular-weight regime. The error bars represent standard deviations of the measurements.

and the second term dominates. The values obtained for the empirical parameters, a and b, are 1.45×10^{-4} cm^2/s and 1.32, respectively. Equation 9 describes well the molecular weight dependence of the diffusion coefficient in DMPC bilayers, as shown in Fig. 3 *a*.

Molecular weight dependence of lateral diffusion in DMPC/cholesterol lipid bilayers

Fig. 3 *b* shows a plot of the diffusion coefficients of the nine fluorescent probes in DMPC/cholesterol bilayers versus the probe molecular weight. Similar to the results obtained in DMPC bilayers (Fig. 3 *a*), the diffusion coefficients initially decrease rapidly with increasing probe molecular weight, whereas the values for probes larger than ~500 Da decrease at a more moderate rate. The fastest probe in this system, DACM, diffuses 4.2-fold faster than the slowest probe, NBD-Chol. This increase suggests that the molecular weight dependence of diffusion in DMPC/cholesterol is greater than that in DMPC, for which a 2.4-fold increase is found. For SCE lipids this dependence is even greater, as discussed in the following section. The error of the DACM diffusion coefficient (SD 26%) is larger than that of the other probes, in part because of the higher noise level resulting from the photostability of the probe, as discussed above.

The diffusion coefficient of BOD in DMPC/cholesterol, 2.33×10^{-8} cm^2/s, lies below the expected trend (Fig. 3 *b*), in contrast to the results for DMPC shown in Fig. 3 *a*. The reason for the observed discrepancy is not clear. One possible explanation is that the localization of BOD within the bilayer is different from that of the other probes. In fact, small solutes are not evenly distributed across lipid bilayers but exhibit characteristic concentration profiles that depend on the chemical–physical properties of the solute (Bassolino-Klimas et al., 1993; Gawrisch and Janz, 1991; Marqusee and Dill, 1986; Martel et al., 1993; White et al., 1981; Alper and Stouch, 1995; Dix et al., 1978; Marrink and Berendsen, 1994). The diffusion coefficient of a given solute has been shown to vary with its location in the bilayer. However, this explanation does not account for the observed behavior because a given probe (namely, BOD) is likely to have similar bilayer distribution profiles in DMPC and DMPC/cholesterol systems. A second possible explanation is that cholesterol causes BOD to segregate laterally, as previously reported for proteins in DMPC bilayers (Cherry et al., 1980; Nigg and Cherry, 1979). However, it is not clear why BOD would segregate while the other probes did not, particularly given the low concentrations of the probes in the bilayers (0.1 mol%). A third possible explanation is that the diffusion coefficient scales more precisely with molecular area or molecular volume than with molecular weight. However, inasmuch as the sizes of the probes do not change from one lipid system to the other, this explanation does not account for the qualitative variations in the profiles observed in DMPC (Fig. 3 *a*) and DMPC/cholesterol (Fig. 3 *b*). Such variations suggest the need for more-sophisticated models to describe small-solute diffusion in lipid bilayer systems.

Fig. 3 *b* also shows the results of a least-squares regression of Eq. 9 applied to the DMPC/cholesterol diffusion data. We used 3.9 *P* as the bilayer viscosity, η_o, rather than the value of 0.75 *P* that describes DMPC bilayers, to account for the lower values of the diffusion coefficients. This viscosity was determined such that the ratio of the diffusion coefficients (calculated with Eq. 8) of the largest probe, NBD-PE, in DMPC and DMPC/cholesterol was the same as the experimentally measured ratio of 4.3. The values of the empirical parameters, a and b, are 2.32×10^{-2} cm^2/s and 2.48, respectively. Fig. 3 *b* shows that Eq. 9 describes well the molecular weight dependence of the diffusion coefficient in DMPC/cholesterol bilayers.

Molecular weight dependence of lateral diffusion in SCE lipid bilayers

The diffusion coefficients of DACM, BOD, NBD-dioct, NBD-dihexdec, and NBD-Chol in SCE lipid bilayers are plotted in Fig. 3 *c* versus the probe molecular weight. As observed in DMPC and DMPC/cholesterol bilayers, the diffusion coefficients in SCE bilayers decrease with increasing probe molecular weight. The values shown in Fig. 3 *c*, however, are considerably lower than those for diffusion in DMPC and DMPC/cholesterol, by average ratios of 15 ($\pm$7) and 3.4 ($\pm$1.4), respectively. The ratio of the largest diffusion coefficient in SCE bilayers (that of DACM) to the smallest (that of NBD-dihexdec) is 7.6, which is considerably greater than the corresponding ratios in DMPC (2.4) and DMPC/cholesterol (4.4). Although this ratio constitutes only a rough indication of the molecular weight dependencies of diffusion in these three lipid systems, it does show that those lipid systems characterized by lower diffusion coefficients exhibit greater molecular weight dependencies. The reason for this may be that the diffusion coefficients of the smallest compounds (such as the molecular gas, O_2) are less sensitive to the effective viscosity of the system than are those of the larger compounds, and hence that the diffusion coefficient in more "viscous" systems (SCE > DMPC/cholesterol > DMPC) increases to a greater extent with decreasing solute molecular weight. This conjecture is supported by literature data for a variety of systems, as discussed below.

The molecular weight dependence given by Eq. 9 nicely describes the SCE bilayer experimental data (Fig. 3 *c*). The value for the effective bilayer viscosity, η_o, used in this equation is 21.3 *P*. This viscosity was determined such that the ratio of the diffusion coefficients (calculated with Eq. 8) of the two largest probes in SCE (NBD-dihexdec and NBD-Chol) with their diffusion coefficients in DMPC was the same as the experimentally measured ratio of 24. For reference, note that the viscosity of glycerol is 11 *P* at 20°C (Bird et al., 1960). Caution should be exercised in interpret-

ing these bilayer viscosities and in making comparisons with the viscosities of bulk fluids, such as glycerol. Whereas the diffusion of large probes can be modeled in terms of a viscosity, this property has yet to be linked with the chemical structure of the lipids and hence represents an effective property of the bilayer (see Clegg and Vaz (1985) for a thorough critique of bilayer hydrodynamic theories). Free-area/free-volume theories can also effectively describe diffusion of lipid probes in bilayers under a variety of conditions (Almeida et al., 1992). The values of the empirical parameters a and b for the SCE diffusion data obtained with Eq. 9 are 13 cm^2/s and 3.75, respectively. The value of b, the exponent of Eq. 9, 3.75 (± 0.83), is in agreement with the exponent previously obtained for describing SC permeabilities, 4.6 (Anderson and Raykar, 1989).

The predominant diffusion coefficient describing BOD-Chol diffusion in SCE bilayers, 1.25×10^{-9} cm^2/s, corresponds to 78% of the diffusing species, as determined with the two-diffusion-coefficient model (Eq. 6). As BOD-Chol has a molecular weight of 787 Da, this value is consistent with the molecular weight dependence shown in Fig. 3 *c*. Interestingly, the diffusion coefficient of the smaller population, 1.59×10^{-8} cm^2/s, is essentially the same as that of BOD-Chol in DMPC/cholesterol, 1.69×10^{-8} cm^2/s. Various physical explanations have been proposed to rationalize the results of polymodal models in other complex bilayer systems, including 1) "fast" probe diffusion along structural defects or partially disordered bands in single-component, gel-phase DMPC bilayers (Derzko and Jacobson, 1980; Schneider et al., 1983), 2) kinetic binding of proteins coupled with lateral diffusion (Huang et al., 1994), and 3) probe distribution between the inner and outer leaflets of erythrocyte membranes (Schroeder et al., 1991). However, these explanations are not applicable to diffusion in SCE lipids because 1) the DMPC gel phase represents a special case in that it is a highly ordered, single-component system, the transport characteristics of which are not observed even in two-component lipid systems (Almeida et al., 1992), let alone in SCE lipids, 2) there is no physical basis for assuming that there is kinetic binding in the present study, as there was in previous studies with proteins (Huang et al., 1994), and 3) there is no evidence that SCE bilayer leaflets exhibit the anisotropy observed in erythrocytes. Therefore, it is not clear whether the results for BOD-Chol in SCE, which suggest bimodal diffusion, are correctly capturing probe diffusion in two distinct domains of SCE lipids or whether the results could be induced by some other mechanism.

Experiments on BOD-FA and BOD-Cer diffusion in SCE lipids did not exhibit the discernible exponential decays observed with the other probes and lipid systems, such as those shown in Fig. 2, although qualitative observations of the bleach spots revealed that there was fluorescence recovery on a time scale similar to those of the other probes in SCE lipids (~20–~30 s). This apparent failure of the data to collapse into a discernible pattern when plotted against the frequency-scaled time indicates that phenomena other than simple, homogeneous diffusion are affecting the recovery process. In contrast, qualitative observations of the NBD-PE bleach spot in SCE lipids revealed that there was very little fluorescence recovery, even after more than 10 min. Similarly, the noise of the data in the NBD-PE decay profiles was greater than any recovery that took place. One possible explanation for these results is that there are disclinations or domain boundaries within SCE lipid bilayers and that a given probe has to cross such boundaries to reach more-distant parts of the lipid structure. These crossings may involve transbilayer diffusion, also referred to as flip-flop for phospholipid molecules. Large, long-tailed lipids exhibit great difficulty in crossing bilayers (Homan and Pownall, 1988; Lipka et al., 1991), and hence their recovery in these experiments could be significantly hindered by such boundary crossings. This conjecture could explain the results obtained for BOD-FA, BOD-Cer, and NBD-PE in SCE lipids. An analogous finding was made by Kitson et al. (1994), who examined palmitic acid in human stratum corneum, using deuterium nuclear magnetic resonance, and concluded that the diffusion of palmitic acid effectively does not occur. In contrast, small, lipophilic compounds have been shown to diffuse readily across lipid bilayers (Lieb and Stein, 1969), suggesting that boundary crossings in SCE lipids would not play a significant role in the diffusive recoveries of such probes as DACM, BOD, NBD-dioct, and NBD-dihexdec. Cholesterol is also able to diffuse across bilayers much better than phospholipid molecules (Bittman, 1993), suggesting that NBD-Chol and BOD-Chol are similarly unhindered by any potential domain boundaries in SCE lipids. Hence, the experimental observations of the nine probes in SCE lipids are at least in qualitative agreement with this mechanism, although additional studies are needed to elucidate these issues fully.

The transport of molecular oxygen in human stratum corneum and model SC lipids has been examined by electron paramagnetic resonance spectroscopy (Hatcher and Plachy, 1993). The effective diffusion coefficient in the SC, 3×10^{-7} cm^2/s, was not corrected for SC tortuosity. Hence the diffusion coefficient measured in the model SC lipids, 2×10^{-6} cm^2/s, represents a better estimation of the true oxygen diffusion coefficient. This relatively large diffusion coefficient illustrates the significant molecular weight dependence of diffusion in the very low-molecular-weight regime (<200 Da).

Comparison of the lateral diffusion coefficient–molecular weight dependence of small probes in SCE and model lipid bilayer systems

The probes examined in this study exhibit increasing lateral diffusion coefficients with decreasing probe molecular weight, down to 223 Da (DACM) (Fig. 3). The extent to which this trend continues for even smaller probes cannot be discerned from these data, nor is it likely to be determined with the FRAP technique because of the lack of

smaller (<223 Da), lipophilic, fluorescent probes that can absorb and emit light at appropriate wavelengths. Fortunately, lateral diffusion coefficients for several small molecules have been determined by other techniques. A summary of literature values of various lipid and nonlipid probes in DMPC fluid bilayers ($T > T_m$) are shown in Table 2. Table 2 also shows the lateral diffusion coefficients corrected to 30°C by use of the activation energies reported in the same reference in which the diffusion coefficients are reported or by use of the typical value of 7.4 kcal/mol. 7.4 kcal/mol is the average of the activation energies of diffusion of 1-methylpyrene [7.0 kcal/mol (Van den Zegel et al., 1984)], NBD-PE [8.1 kcal/mol (Almeida et al., 1992) and 6.9 kcal/mol (Chang et al., 1981)], and 3,3′-dioctadecyloxacarbocyanine iodide [7.6 kcal/mol (Derzko and Jacobson, 1980)]. Table 2 illustrates the sparsity of lateral diffusion measurements of small probes in DMPC and the lipid nature of the majority of these probes. Nevertheless, DMPC is one of the most studied lipid bilayer systems; hence these data provide one of the clearest portraits of small-probe lateral diffusion (Table 2).

Lateral diffusion coefficients, including both our data (Table 1; corrected to 30°C using an activation energy of 7.4 kcal/mol) and those from the literature (Table 2), are shown in Fig. 4 as a function of probe molecular weight. The top curve in Fig. 4 represents the results of a least-squares regression using Eq. 9 to all the DMPC data reported in Tables 2 and 3 and describes the data well. Also shown in this figure are our results for probe diffusion in DMPC/cholesterol (Table 1) and SCE (Table 3) lipid bilayer systems as well as literature values for diffusion in DMPC/cholesterol 40–50 mol% (NBD-PE values are listed in the Results; the diffusion coefficient for molecular oxygen was determined in the same manner as that for molecular oxygen in DMPC bilayers (see Table 2)) and in SCE (molecular oxygen, discussed above). The middle and bottom curves in Fig. 4 represent the regressions using Eq. 9 of the total data sets for the DMPC/cholesterol and the SCE lipid systems, respectively, and describe these data reasonably well. As the diffusion of small and of large solutes is not generally considered together, because of the solutes' different mechanisms of diffusion, it is remarkable that a two-parameter empirical equation (Eq. 9) is able to effectively describe the data presented in Fig. 4. These findings suggest the need for additional study of the fundamental nature of lateral diffusion in lipid bilayers.

The lateral diffusion coefficients for probes smaller than ~200 Da increase by orders of magnitude in DMPC, DMPC/cholesterol, and SCE bilayer systems (Fig. 4) (note that the value for molecular oxygen in DMPC, 1.8×10^{-5} cm^2/s, is off the scale). This suggests that the 2.4-fold to 7-fold increases observed for DACM (223 Da) over those of larger probes in DMPC, DMPC/cholesterol, and SCE (Fig. 3) represent the beginnings of the low-molecular weight regime that is characterized by this strong molecular weight dependence. Diffusion experiments performed in other single-component phospholipid bilayer systems support the findings in Fig. 4 that small probes (molecular weights of less than ~200 Da) diffuse very rapidly relative to larger probes. Dix et al. (1978) examined diffusion of four small probes in dipalmitoyl-lecithin bilayers, using electron spin-resonance spectroscopy at 50°C: di-*t*-butyl nitroxide (144 Da), 2,2,6,6-tetramethylpiperidine-1-oxyl (TEMPO, 156 Da), carbonyl-TEMPO (170 Da), and benzoyloxy-TEMPO (276 Da). Their reported diffusion coefficients, 1.0×10^{-6}, 0.9×10^{-6}, 0.7×10^{-6}, and 0.6×10^{-6} cm^2/s, respec-

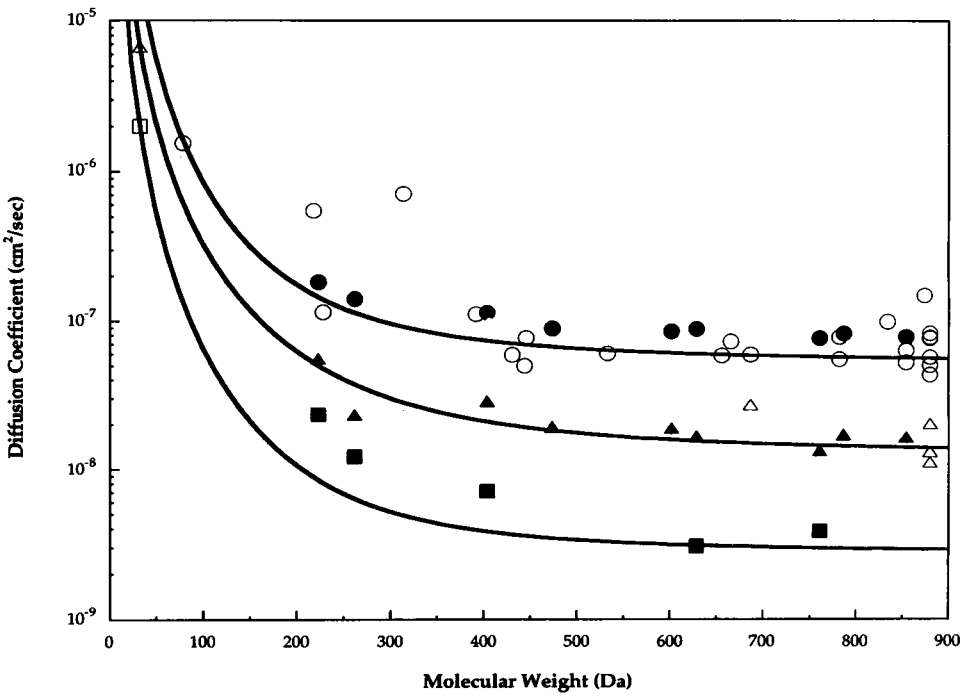

FIGURE 4 Comparisons of the dependencies of lateral diffusion coefficients on molecular weight in DMPC fluid phase bilayers (●, ○), DMPC/cholesterol (40–50 mol% cholesterol) bilayers (▲, △), and SCE bilayers (■, □). ●, ▲, ■, Measurements presented in this paper; ○, △, □, literature data (see Table 2 for details on the DMPC literature data and the text for details on the DMPC/cholesterol and SCE literature data). All DMPC data points were corrected to 30°C (see Table 2 for details). The curves are the results of least-squares regressions of the semiempirical model (Eq. 9) to the combined data sets for these lipid systems, using T = 30°C and η_o = 0.75, 3.9, 21.3 *P* for the effective viscosities of DMPC, DMPC/cholesterol, and SCE bilayers, respectively.

tively, agree very well with the trend shown in Fig. 4 for DMPC bilayers. Likewise, the diffusion coefficient of pyrene (202 Da) measured in dipalmitoylphosphatidylcholine bilayers by the fluorescence decay technique, 1.2×10^{-6} cm^2/s at 50°C, is also in good agreement with the trend of DMPC in Fig. 4 (Daems et al., 1985).

Whereas the molecular weight dependencies for DMPC, DMPC/cholesterol, and SCE lipid bilayer systems appear to be analogous (Fig. 4), it is still not clear what simple model bilayer system, if any, constitutes a reasonable model of SCE bilayers. The results in Figs. 3 and 4 suggest that DMPC is not a quantitatively accurate model of SCE bilayers, as their diffusion coefficients differ by an average of 15-fold. Diffusion coefficients in DMPC/cholesterol and SCE bilayers also differ, but only by an average factor of 3. Several other findings suggest that this difference may not be significant and that DMPC/cholesterol bilayers may be a reasonable model of SCE bilayers. First, a comparison of SCE diffusion data with that of gel-phase ($T < T_m$) DMPC bilayers, which is another potential model of the SCE system, suggests dramatic differences. For example, the average NBD-PE diffusion coefficient in gel-phase DMPC bilayers ($17.5 \leq T \leq 20.5$°C) is 1.6×10^{-10} cm^2/s (Balcom and Petersen, 1993; Chang et al., 1981; Fahey and Webb, 1978; Rubenstein et al., 1979; Smith and McConnell, 1978; Wu et al., 1977), which is 100-fold lower than that in DMPC/cholesterol bilayers (Table 1), corresponding to a 30-fold difference with diffusion in SCE bilayers. Two recent studies of the structural aspects of SCE bilayers have also noted striking similarities between SCE lipids and phospholipid/cholesterol bilayers (Kitson et al., 1994; Ongpipattanakul et al., 1994), again suggesting that SCE bilayers may be reasonably modeled by DMPC/cholesterol bilayers.

The importance of lateral diffusion to the macroscopic stratum corneum permeability has yet to be elucidated, in large part because of the absence of a clear understanding of the nature of small-solute diffusion in lipid bilayers. The results and analysis presented in this paper, which establish the magnitude of diffusion in SCE lipids as well as the qualitative molecular weight dependence of lateral diffusion, are an important step in this direction. Further studies are currently under way to evaluate the contribution of lateral diffusion to transdermal transport at both qualitative and quantitative levels.

This research was supported by National Institutes of Health Grant GM44884. M.E.J is grateful to Eastman Kodak Company for the award of a graduate fellowship. D.A.B was supported by the Whitaker Foundation. D.E.G acknowledges receipt of National Institutes of Health Grant HL-32854. R.K.J acknowledges receipt of National Cancer Institute Grant R35 CA 56591.

REFERENCES

Almeida, P. F. F., W. L. C. Vaz, and T. E. Thompson. 1992. Lateral diffusion in the liquid phases of dimyristoylphosphatidylcholine/cholesterol lipid bilayers: a free-volume analysis. *Biochemistry.* 31: 6739–6747.

Alper, H. E., and T. R. Stouch. 1995. Orientation and diffusion of a drug analogue in biomembranes: molecular dynamics simulations. *J. Phys. Chem.* 99:5724–5731.

Anderson, B. D., W. I. Higuchi, and P. V. Raykar. 1988. Heterogeneity effects on permeability-partition coefficient relationships in human stratum corneum. *Pharm. Res.* 5:566–573.

Anderson, B. D., and P. V. Raykar. 1989. Solute structure-permeability relationships in human stratum corneum. *J. Invest. Dermatol.* 93: 280–286.

Balcom, B. J., and N. O. Petersen. 1993. Lateral diffusion in model membranes is independent of the size of the hydrophobic region of molecules. *Biophys. J.* 65:630–637.

Bassolino-Klimas, D., H. W. Alper, and T. R. Stouch. 1993. Solute diffusion in lipid bilayer membranes: an atomic level study by molecular dynamics simulations. *Biochemistry.* 32:12,624–12,637.

Berk, D. A., F. Yuan, M. Leunig, and R. K. Jain. 1993. Fluorescence photobleaching with spatial Fourier analysis: measurement of diffusion in light-scattering media. *Biophys. J.* 65:2428–2436.

Bird, R. B., W. E. Stewart, and E. N. Lightfoot. 1960. Transport Phenomena. John Wiley & Sons, New York.

Bittman, R. 1993. A review of the kinetics of cholesterol movement between donor and acceptor bilayer membranes. *In* Cholesterol in Membrane Models. L. Finegold, editor. CRC Press, Boca Raton, FL. 45–65.

Bouwstra, J. A., G. S. Gooris, J. A. v. d. Spek, and W. Bras. 1991. Structural investigations of human stratum corneum by small-angle X-ray scattering. *J. Invest. Dermatol.* 97:1005–1012.

Chang, C.-H., H. Takeuchi, T. Ito, K. Machida, and S. Ohnishi. 1981. Lateral mobility of erythrocyte membrane proteins studied by the fluorescence photobleaching recovery technique. *Biochemistry.* 90: 997–1004.

Cherry, R. J. 1979. Rotational and lateral diffusion of membrane proteins. *Biochim. Biophys. Acta.* 559:289–327.

Cherry, R. J., U. Muller, C. Holenstein, and M. P. Heyn. 1980. Lateral segregation of proteins induced by cholesterol in bacteriorhodopsin-phospholipid vesicles. *Biochim. Biophys. Acta.* 596:145–151.

Clegg, R. M., and W. L. C. Vaz. 1985. Translational diffusion of proteins and lipids in artificial lipid bilayer membranes. A comparison of experiment with theory. *In* Progress in Protein-Lipid Interactions. A. Watts and J. J. H. H. M. DuPont, editors. Elsevier Science Publishing Co., Amsterdam. 173–229.

Cooper, E. R., and G. Kasting. 1987. Transport across epithelial membranes. *J. Control. Rel.* 6:23–35.

Daems, D., M. V. d. Zegel, N. Boens, and F. C. D. Schryver. 1985. Fluorescence decay of pyrene in small and large unilamellar L,a-dipalmitoylphosphatidylcholine vesicles above and below the phase transition temperature. *Eur. Biophys. J.* 12:97–105.

Derzko, Z., and K. Jacobson. 1980. Comparative lateral diffusion of fluorescent lipid analogues in phospholipid multibilayers. *Biochemistry.* 19:6050–6057.

Diamond, J. M., and Y. Katz. 1974. Interpretation of nonelectrolyte partition coefficients between dimyristoyl lecithin and water. *J. Membrane Biol.* 17:121–154.

Dix, J. A., D. Kivelson, and J. M. Diamond. 1978. Molecular motion of small nonelectrolyte molecules in lecithin bilayers. *J. Membrane Biol.* 40:315–342.

Fahey, P. F., and W. W. Webb. 1978. Lateral diffusion in phospholipid bilayer membranes and multilamellar liquid crystals. *Biochemistry.* 17: 3046–3053.

Flynn, G. L. 1990. Physiochemical determinants of skin absorption. *In* Principles of Route-to-Route Extrapolation for Risk Assessment. T. R. Gerrity and C. J. Henry, editors. Elsevier Science Publishing Co., New York. 93–127.

Friberg, S. E., and D. W. Osborne. 1985. Small angle x-ray diffraction patterns of stratum corneum and a model structure for its lipids. *J. Disp. Sci. Tech.* 6:485–495.

Galla, H. J., W. Hartmann, U. Theilen, and E. Sackman. 1979. On two-dimensional passive random walk in lipid bilayers and fluid pathways in biomembranes. *J. Membrane Biol.* 48:215–36.

Gawrisch, K., and S. Janz. 1991. The uptake of pristane (2, 6, 10, 14-tetramethylpentadecane) into phospholipid bilayers as assessed by

NMR, DSC, and tritium labeling methods. *Biochim. Biophys. Acta.* 1070:409–418.

Hansch, C., and A. Leo. 1979. Substituent Constants for Correlation Analysis in Chemistry and Biology. John Wiley & Sons, New York.

Hatcher, M. E., and W. Z. Plachy. 1993. Dioxygen diffusion in the stratum corneum: an EPR spin label study. *Biochim. Biophys. Acta.* 1149:73–78.

Homan, R., and H. J. Pownall. 1988. Transbilayer diffusion of phospholipids: dependence on head group structure and acyl chain length. *Biochim. Biophys. Acta.* 938:155–166.

Hou, S. Y. E., A. K. Mitra, S. H. White, G. K. Menon, R. Ghadially, and P. M. Elias. 1991. Membrane structures in normal and essential fatty acid-deficient stratum corneum: characterization by ruthenium tetroxide staining and x-ray diffraction. *J. Invest. Dermatol.* 96:215–223.

Huang, Z., K. H. Pearce, and N. L. Thompson. 1994. Translational diffusion of bovine prothrombin fragment 1 weakly bound to supported planar membranes: measurements by total internal reflection with fluorescence pattern photobleaching recovery. *Biophys. J.* 67:1754–1766.

Johnson, E. M., D. A. Berk, R. K. Jain, and W. M. Deen. 1995b. Diffusion and partitioning of proteins in charged agarose gels. *Biophys. J.* 68: 1561–1568.

Johnson, M. E., D. Blankschtein, and R. Langer. 1995a. Permeation of steroids through human skin. *J. Pharm. Sci.* 84:1144–1146.

Kapitza, H. G., D. A. Ruppel, H. J. Galla, and E. Sackmann. 1984. Lateral diffusion of lipids and glycophorin in solid phosphatidylcholine bilayers: the role of structural defects. *Biophys. J.* 45:577–587.

Kasting, G. B., R. L. Smith, and B. D. Anderson. 1992. Prodrugs for dermal delivery: solubility, molecular size, and functional group effects. *In* Prodrugs: Topical and Ocular Delivery. K. B. Sloan, editor. Marcel Dekker, New York. 117–161.

Kitson, N., J. Thewalt, M. Lafleu, and M. Bloom. 1994. A model membrane approach to the epidermal permeability barrier. *Biochemistry.* 33:6707–6715.

Lampe, M. A., A. L. Burlingame, J. Whitney, M. L. Williamss, B. E. Brown, E. Roitman, and P. M. Elias. 1983. Human stratum corneum lipids: characterization and regional variations. *J. Lipid Res.* 24: 120–130.

Lange-Lieckfeldt, R., and G. Lee. 1992. Use of a model lipid matrix to demonstrate the dependence of the stratum corneum's barrier properties on its internal geometry. *J. Control. Rel.* 20:183–194.

Lieb, W. R., and W. D. Stein. 1969. Biological membranes behave as non-porous polymeric sheets with respect to the diffusion of non-electrolytes. *Nature (London).* 224:240–243.

Lieb, W. R., and W. D. Stein. 1986. Non-Stokesian nature of transverse diffusion within human red cell membranes. *J. Membrane Biol.* 92: 111–119.

Lipka, G., J. A. F. O. d. Kamp, and H. Hauser. 1991. Lipid asymmetry in rabbit intestinal brush border membrane as probed by an intrinsic phospholipid exchange protein. *Biochemistry.* 30:11,828–11,836.

Mabrey, S., and J. M. Sturtevant. 1976. Investigation of phase transitions of lipids and lipid mixtures by high sensitivity differential scanning calorimetry. *Proc. Natl. Acad. Sci. USA.* 73:3862–3866.

Madison, K. C., D. C. Swartzendruber, P. W. Wertz, and D. T. Downing. 1987. Presence of intact intercellular lipid lamellae in the upper layers of the stratum corneum. *J. Invest. Dermatol.* 88:714–718.

Marqusee, J. A., and K. A. Dill. 1986. Solute partitioning into chain molecule interphases: monolayers, bilayer membranes, and micelles. *J. Chem. Phys.* 85:434–444.

Marrink, S., and H. J. C. Berendsen. 1994. Simulation of water transport through a lipid membrane. *J. Phys. Chem.* 98:4155–4168.

Martel, P., A. Makriyannis, T. Mavromoustakos, K. Kelly, and K. R. Jeffrey. 1993. Topography of tetrahydrocannabinol in model membranes using neutron diffraction. *Biophys. Biochem. Acta.* 1151:51–58.

Nigg, E. A., and R. J. Cherry. 1979. Influence of temperature and cholesterol on the rotational diffusion of band 3 in the human erythrocyte membrane. *Biochemistry.* 18:3457–3465.

Ongpipattanakul, B., M. L. Francoeur, and R. O. Potts. 1994. Polymorphism in stratum corneum lipids. *Biochim. Biophys. Acta.* 1190: 115–122.

Paprica, P. 1994. Evidence for a continuum model of diffusion in lipid membranes. Ph.D. dissertation, University of Western Ontario.

Peters, R., and R. J. Cherry. 1982. Lateral and rotational diffusion of bacteriorhodopsin in lipid bilayers: experimental test of the Saffman-Delbrück equations. *Proc. Natl. Acad. Sci. USA.* 79:4317–4321.

Potts, R. O., and R. H. Guy. 1992. Predicting skin permeability. *Pharm. Res.* 9:663–669.

Rubenstein, J. L., B. A. Smith, and H. M. McConnell. 1979. Lateral diffusion in binary mixtures of cholesterol and phosphatidylcholines. *Proc. Natl. Acad. Sci. USA.* 76:15–18.

Saffman, P. G., and M. Delbrück. 1975. Brownian motion in biological membranes. *Proc. Natl. Acad. Sci. USA.* 72:3111–3113.

Scheuplein, R. J., and I. H. Blank. 1971. Permeability of the skin. *Physiol. Rev.* 51:702–747.

Schroeder, F., G. Nemecz, W. G. Wood, C. Joiner, G. Morrot, M. Ayraut-Jarrier, and P. F. Devaux. 1991. Transmembrane distribution of sterol in the human erythrocyte. *Biochim. Biophys. Acta.* 1066:183–192.

Smith, B. A., and H. M. McConnell. 1978. Determination of molecular motion in membranes using periodic pattern photobleaching. *Proc. Natl. Acad. Sci. USA.* 75:2759–2763.

Subczynski, W., J. S. Hyde, and A. Kusumi. 1991. Effect of alkyl chain unsaturation and cholesterol intercalation on oxygen transport in membranes: a pulse ESR spin labeling study. *Biochemistry.* 30: 8578–8590.

Tocanne, J. F., L. Dupou-Cezanne, A. Lopez, and J. F. Tournier. 1989. Lipid lateral diffusion and membrane organization. *FEBS Lett.* 257: 10–16.

Tsay, T. T., and K. A. Jacobson. 1991. Spatial Fourier analysis of video photobleaching measurements: principles and optimization. *Biophys. J.* 60:360–368.

Van den Zegel, M., N. Boens, and F. C. D. Schryver. 1984. Fluorescence decay of 1-methylpyrene in small unilamellar L-a-dimyristoylphosphatidylcholine vesicles. A temperature and concentration dependence study. *Biophys. Chem.* 20:333–345.

Vaz, W. L. C., R. M. Clegg, and D. Hallmann. 1985. Translational diffusion of lipids in liquid crystalline phase phosphatidylcholine multibilayers. A comparison of experiment with theory. *Biochemistry.* 24:781–786.

Vaz, W. L. C., F. Goodsaid-Salduondo, and K. Jacobson. 1984. Lateral diffusion of lipids and proteins in bilayer membranes. *FEBS Lett.* 174: 199–207.

Vaz, W. L. C., E. C. C. Melo, and T. E. Thompson. 1989. Translational diffusion and fluid domain connectivity in a two-component, two-phase phospholipid system. *Biophys. J.* 56:869–876.

Vaz, W. L. C., E. C. C. Melo, and T. E. Thompson. 1990. Fluid phase connectivity in an isomorphous, two-component, two-phase phosphatidylcholine bilayer. *Biophys. J.* 58:273–275.

Weast, R. C. 1975. Handbook of Chemistry and Physics. CRC Press, Cleveland, OH.

White, S. H., G. I. King, and J. E. Cain. 1981. Location of hexane in lipid bilayers by neutron diffraction. *Nature (London).* 290:161–63.

Wright, L. L., A. G. Palmer, and N. L. Thompson. 1988. Inhomogeneous translational diffusion of monoclonal antibodies on phospholipid Langmuir-Blodgett films. *Biophys. J.* 54:463–470.

Wu, E., K. Jacobson, and D. Papahadjopoulos. 1977. Lateral diffusion in phospholipid multibilayers measured by fluorescence recovery after photobleaching. *Biochemistry.* 16:3936–41.